SHUTTLE VERTICAL FIN FLOWFIELD BY THE DIRECT SIMULATION MONTE CARLO METHOD

J.E. Hueser and F.J. Brock

Old Dominion University

L.T. Melfi

NASA Langley Research Center

Abstract. The flow properties in a model flowfield, simulating the shuttle vertical fin, have been determined using the Direct Simulation Monte Carlo method. The case analyzed corresponds to an orbit height of 225 km with the freestream velocity vector orthogonal to the fin surface. Contour plots of the flowfield distributions of density, temperature, velocity and flow angle are presented. The results also include mean molecular collision frequency (which reaches $60\ s^{-1}$ near the surface), collision frequency density (approaches $7 \times 10^{18}\ m^{-3}\ s^{-1}$ at the surface) and the mean-free-path (19 m at the surface).

Introduction

The glow that has been observed on shuttle flights has prompted much speculation about possible source mechanisms. A definition of the flowfield properties in the glow space should provide information which may assist in resolving the applicable physical mechanisms. The shuttle vertical fin was taken as a representative surface and a geometrically similar flow model was constructed. The flow properties were determined using the Direct Simulation Monte Carlo method [Bird, 1976]. The vertical fin was modeled as a disk having an 8 m radius, oriented with its surface-normal antiparallel to the freestream velocity vector, and embedded in an axisymmetric flowfield. The geometry and the computational cell distribution of the Monte Carlo flowfield are shown in Figure 1. The forward surface of the disk is located at x = -0.01 m and the flow is in the + x direction. The boundary conditions along the forward (x = -20 m) and outer flowfield boundaries correspond to the incident flux density of an equilibrium gas (atmosphere at orbit height) drifting at 7.76 km/s. The disk surface temperature was set at 150 K and a diffuse reflection law was used. Vacuum conditions were applied to the downstream side of the aft boundary (x = 8 m). The freestream density $n = 0.4915 \times 10^{16}\ m^{-3}$, temperature T = 1090 K, and composition were taken from the properties of the atmosphere [Jacchia, 1977] at an orbit height of 225 km. The gas composition and molecular properties used are given in Table 1. The variable hard sphere molecular model [Bird, 1981] was used with a viscosity coefficient temperature exponent of 0.75.

Results and Discussion

The flowfield number density (m^{-3}) distribution is given by the contours displayed in Figure 1. The flowfield forward boundary (x = -20 m) is only 2.5 disk radii upstream of the disk which yields a substantial discontinuity between flowfield properties at the forward boundary and freestream properties (the number density at the forward boundary is 1.7×10^{16} m^{-3} while the freestream density at the forward boundary is 0.49×10^{16} m^{-3}). However, previous results with the Direct Simulation Monte Carlo method indicate that this boundary effect is rather localized and does not substantially influence the results in the vicinity of the disk, The density near the axis and near the forward surface of the disk (the centroid of the nearest cell to the surface is 8 cm upstream) is approximately 2.2×10^{17} m^{-3}, a factor of 44 above the undisturbed freestream density. The density near the aft surface of the disk drops to nearly 10^{12} m^{-3}.

Contours of axial velocity (m/s), radial velocity (m/s) and flow angle (radians) are also given in Figure 1. These results imply that the flow is nearly axial for a few meters near the forward boundary and gradually approaches radial flow near the forward surface of the disk. There is a small region adjacent to the forward surface, near the axis, in which both velocity components are sufficiently small that the flow angle cannot be resolved unambiguously (see noise in flow angle contours). The axial velocity component would coincide with the undisturbed freestream speed well forward of the forward boundary of the flowfield.

The mean translational and internal temperature (K) distributions are given by the contours in Figure 2. The entire flowfield is highly non-equilibrium and thus temperature should be treated with caution. The translational temperature peak is outside (forward) of the flowfield. Both temperatures, of course, approach 150 K at the disk surface.

The mean collision frequency (s^{-1}) and collision frequency density (m^{-3} s^{-1}) distributions are also given in Figure 2. Near the disk forward surface, for r < 6 m, the collision frequency is approximately 63 s^{-1} and the collision frequency density is slightly larger than 6.7×10^{18} m^{-3} s^{-1} . The flow speed in this region is less than 5 m/s, implying that a molecule may experience several collisions before drifting out of the region.

In Figure 3 several of the flow parameters are displayed as functions of x only for r = 0.95 m (near the axis) and in Figure 4 for r = 7.6 m (near the outer edge of the disk), the disk surface is at x = -0.01 m in each subframe. Each displayed function is normalized by its maximum value before plotting. The normalization constants for each curve are written adjacent to the curve label above each subframe. The label definitions are:

ND = number density (m^{-3})
CO = stream speed, mass average (m/s)
TR = translational temperature (K)
TI = internal temperature (K)
VX = axial velocity component (m/s)
VY = radial velocity component (m/s)
FA = flow angle (0 corresponds to $-\pi$ and 1 to $+\pi$)
LB = mean-free-path (m)
NU = molecular mean collision frequency (s^{-1})
NC = mean collision frequency density (m^{-3} s^{-1})

Note the rapid increase in density and both collision frequencies (especially the collision frequency density, curve NC) as the flow approaches the surface, while the mean-free-path decreases rather linearly. The peak of the radial velocity increases by about an order of magnitude between the two figures and moves closer to the surface as r increases. For the outer radial cut (7.6 m) the flow angle approaches $\pi/2$ (0.75 on the ordinate) but along the inner radial cut is always less than $\pi/2$.

The surface parameters along the disk are plotted in Figure 5 as a function of r. The forward surface of the disk lies along the abscissa for the two subframes on the left, with the origin at 0.0 m and the outer edge at r = 8 m and similarly for the two subframes on the right, the aft surface of the disk lies along the abscissa. The upper left subframe gives flux density (m^{-2} s^{-1}) incident on the forward surface for each species (curves F1, F2, F3) and the total (sum over species, curve FD). All four curves are normalized by the peak value of the total flux density; thus, the ordinate gives the relative fraction of the total flux density produced by each species (F1, F2, & F3 correspond to species 1, 2, & 3). The maximum value of the incident flux density for the total and each species is written above the subframe adjacent to each curve label. The lower left subframe gives normalized plots of surface pressure (Pa) (curve PR), surface shear (curve SH), incident power density (W/m^2) (curve PI), and reflected power density (curve PR). The normalization constants for each curve are written adjacent to each curve label above the subframe. The two subframes on the right present the same parameters in the same way for the aft surface of the disk. Note that only species 3 (atomic oxygen) appears. It is quite probable that the lower relative abundance species would appear if the solution had been carried to a substantially larger flow time.

The peak total incident flux density (near r = 0) on the forward surface is 4.1×10^{19} m^{-2} s^{-1} which is about 8% larger than the collisionless value (3.8×10^{19} m^{-2} s^{-1}). On the aft surface (for this particular flow time) the peak total incident flux density is 2×10^{14} m^{-2} s^{-1} (collisionless flow would yield a number orders of magnitude smaller). However, the properties along the aft surface must be regarded as approximate, preliminary estimates due to the very small sample size.

In the Monte Carlo model, each molecular encounter was counted for each molecule until it collided with the forward surface the first time. These data imply that in the mean the total collision probability for a molecule reaching the forward surface the first time is 0.07. If the flowfield length had been sufficiently large to contain the total disturbance produced in the freestream by the disk, this number would have increased, but probably by less than a factor of 2.

There is internal evidence from the Monte Carlo model implying a highly bimodal sample distribution near the forward surface, consisting of high-velocity freestream molecules flowing toward the surface and a low-velocity reflected stream flowing away from the surface. The axial width of the cells near the surface was selected to yield adequate spatial resolution. The total sample in these cells is large but probably consists principally of molecules from the low-velocity stream. Thus, molecules from the high-velocity stream are under sampled due to the small cell width and corresponding short transit time. This would influence the number of molecular encounters computed in the collision routine and thus influence the collision frequency, collision frequency density and mean-free-path. This situation clearly requires a detailed investigation, which is currently under way.

In a broader sense, there appears to be no unambiguous physical interpretation of mean values formed from the very different sample distributions of the two-stream flow encountered in the current problem. Although the primary flow properties are insensitive to this problem and are therefore regarded as an adequate definition of the flow, the collision frequencies should be used with caution.

References

Bird, G. A., Molecular Gas Dynamics, Clarendon Press, 1976.

Bird, G. A., Monte Carlo simulation in an engineering context, Rarefied Gas Dynamics, Progress in Astronautics and Aeronautics, Vol. 74, Part 1, edited by Sam S. Fisher, AIAA, New York, 1981, pp. 239-255.

Jacchia, L. G., Thermospheric temperature, density, and composition: New models, Smithsonian Astrophysical Observatory Special Report 375, 1977.

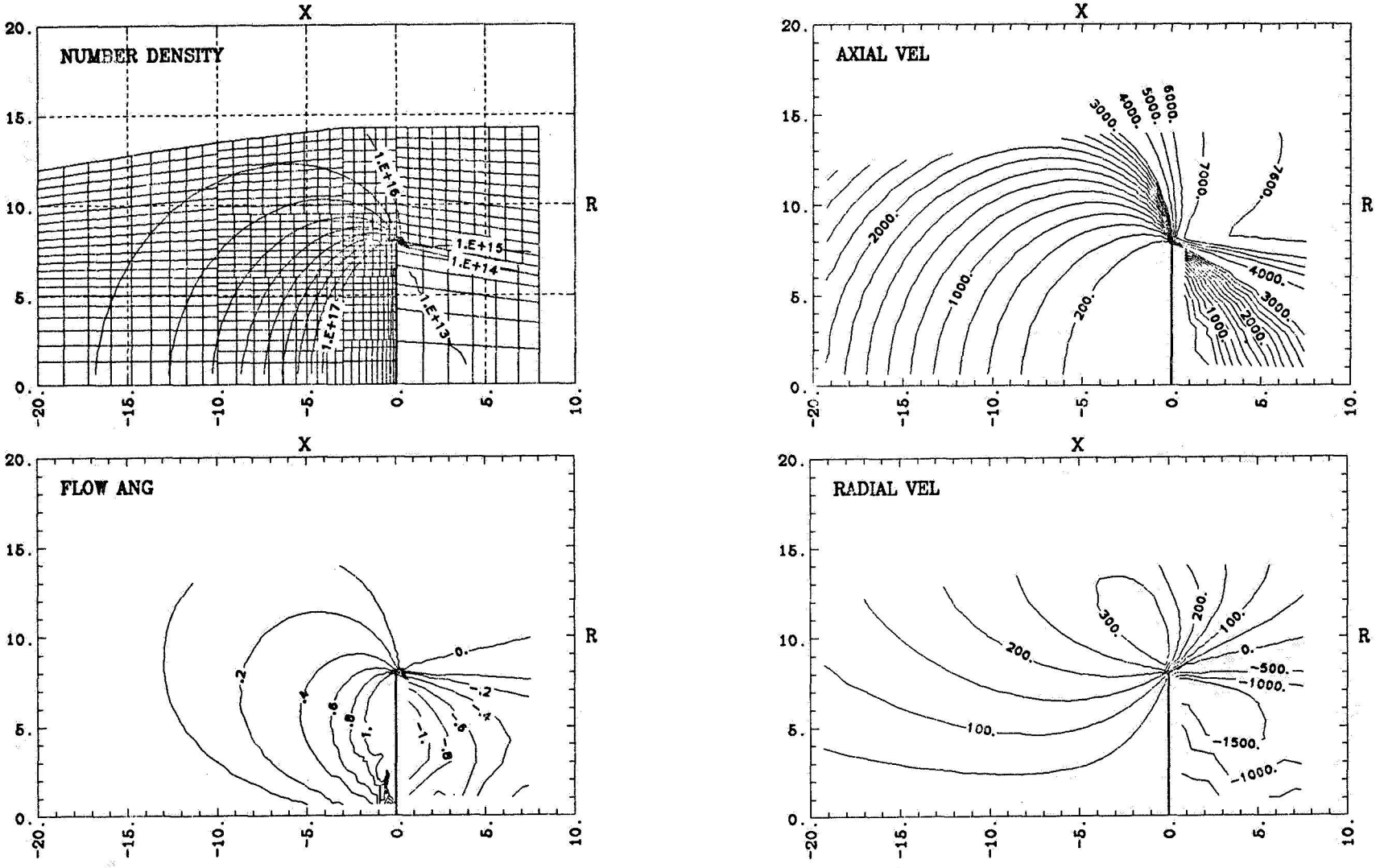

Fig. 1. Contours of flowfield properties, modeled shuttle fin.

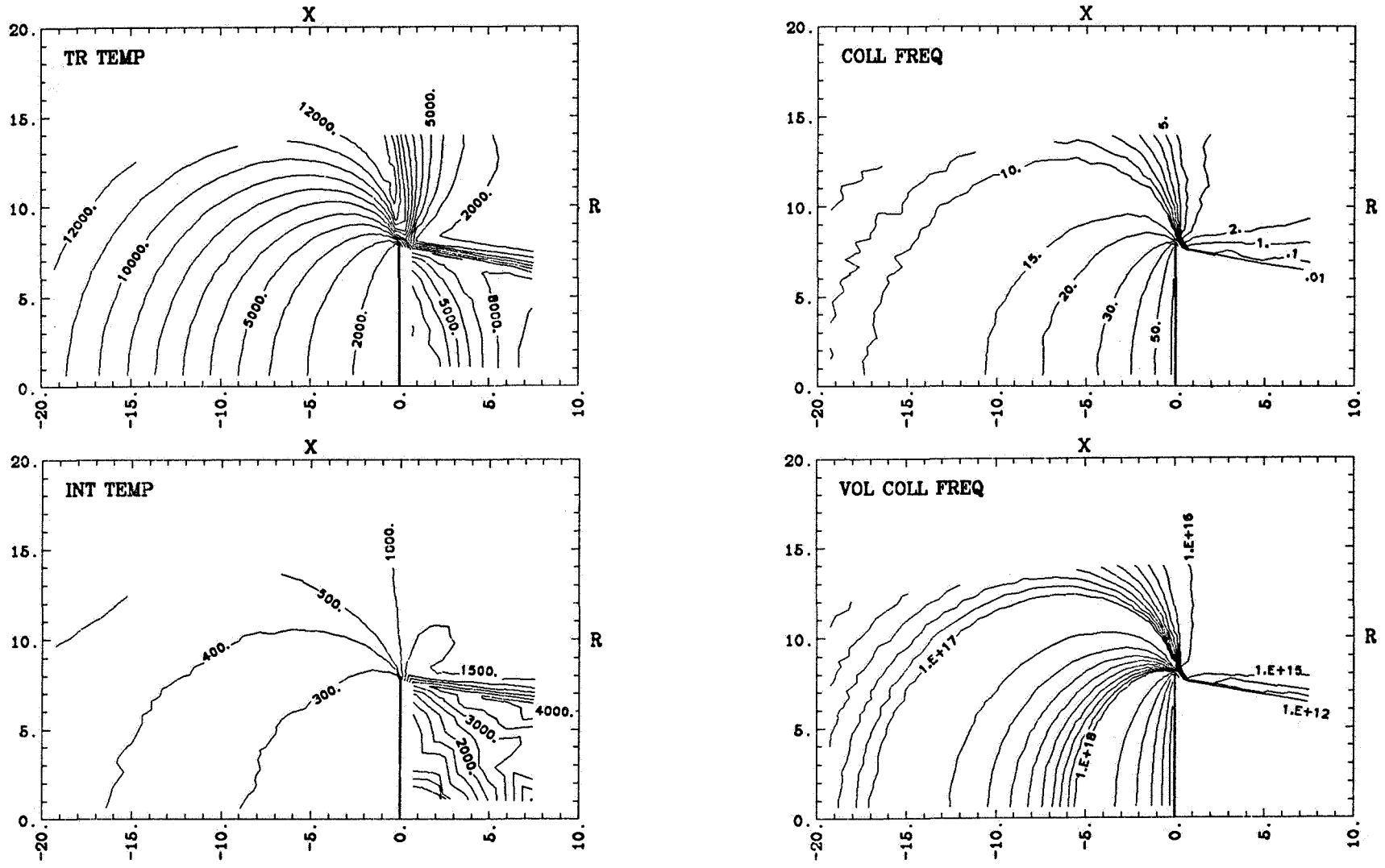

Fig. 2. Contours of flowfield properties, modeled shuttle fin.

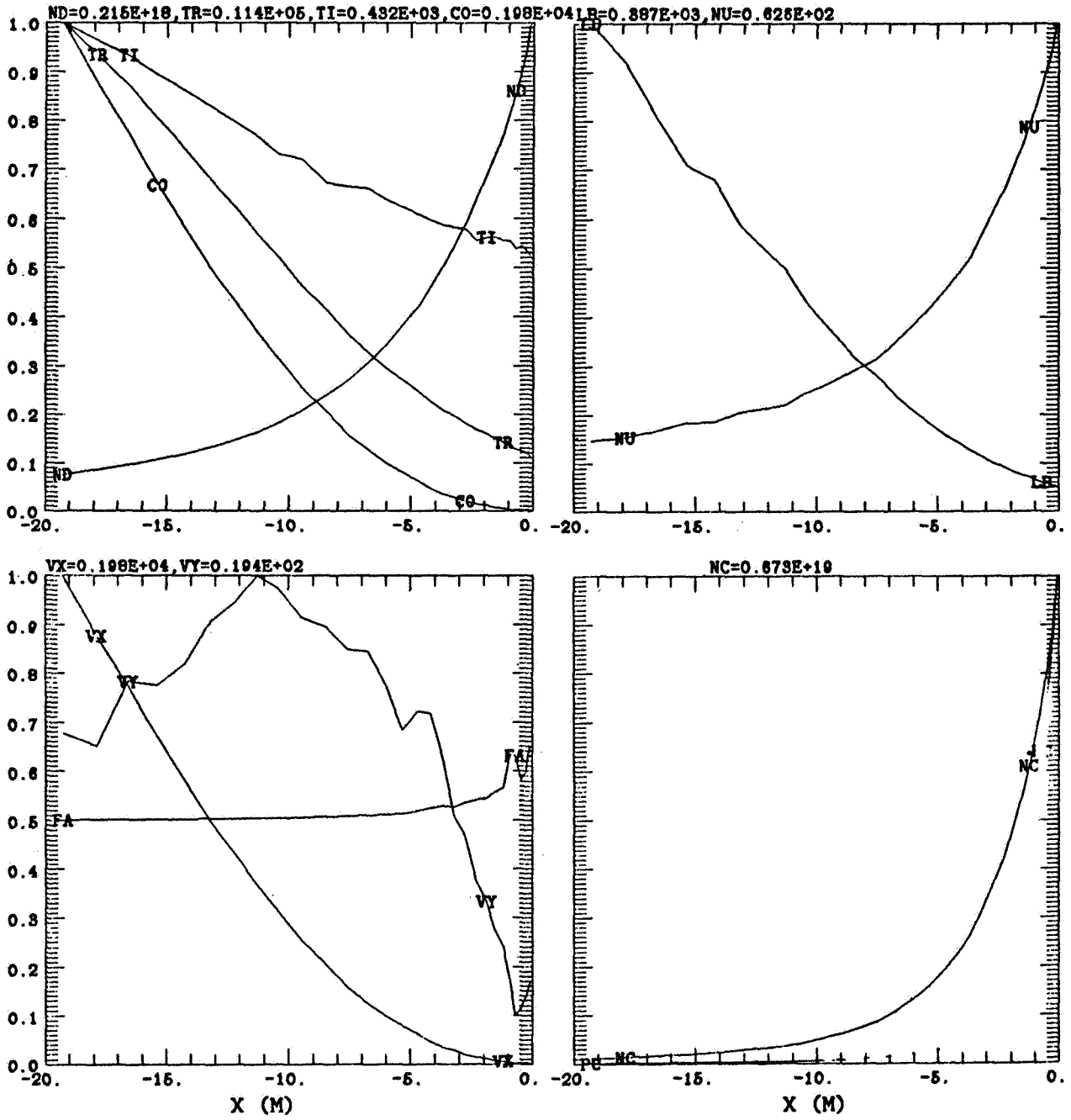

Fig. 3. Flow properties along a fixed radius, r = 0.95 meters. Normalization constants are given above each frame.

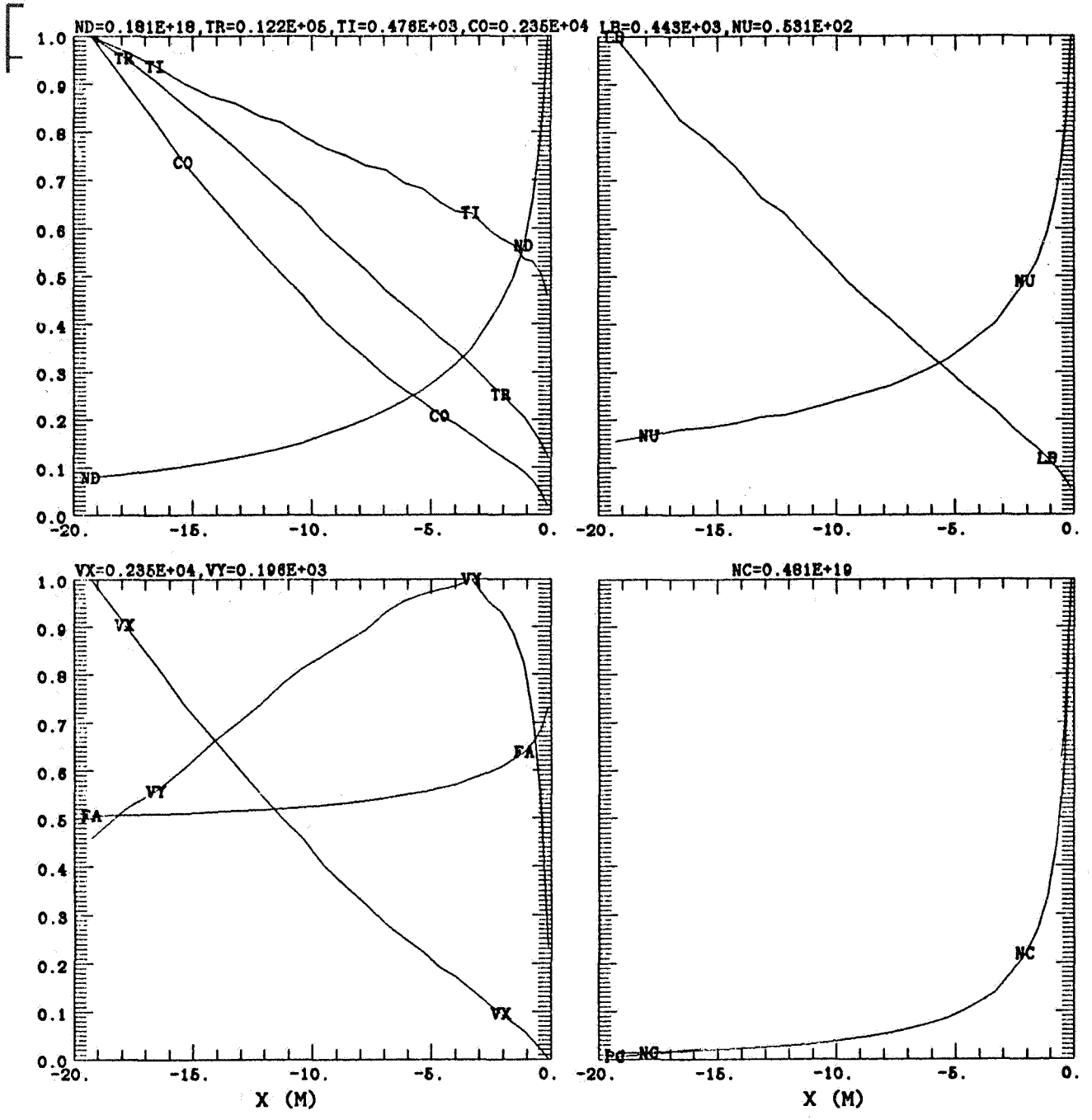

Fig. 4. Flow properties along a fixed radius, r = 7.6 meters. Normalization constants are give above each frame.

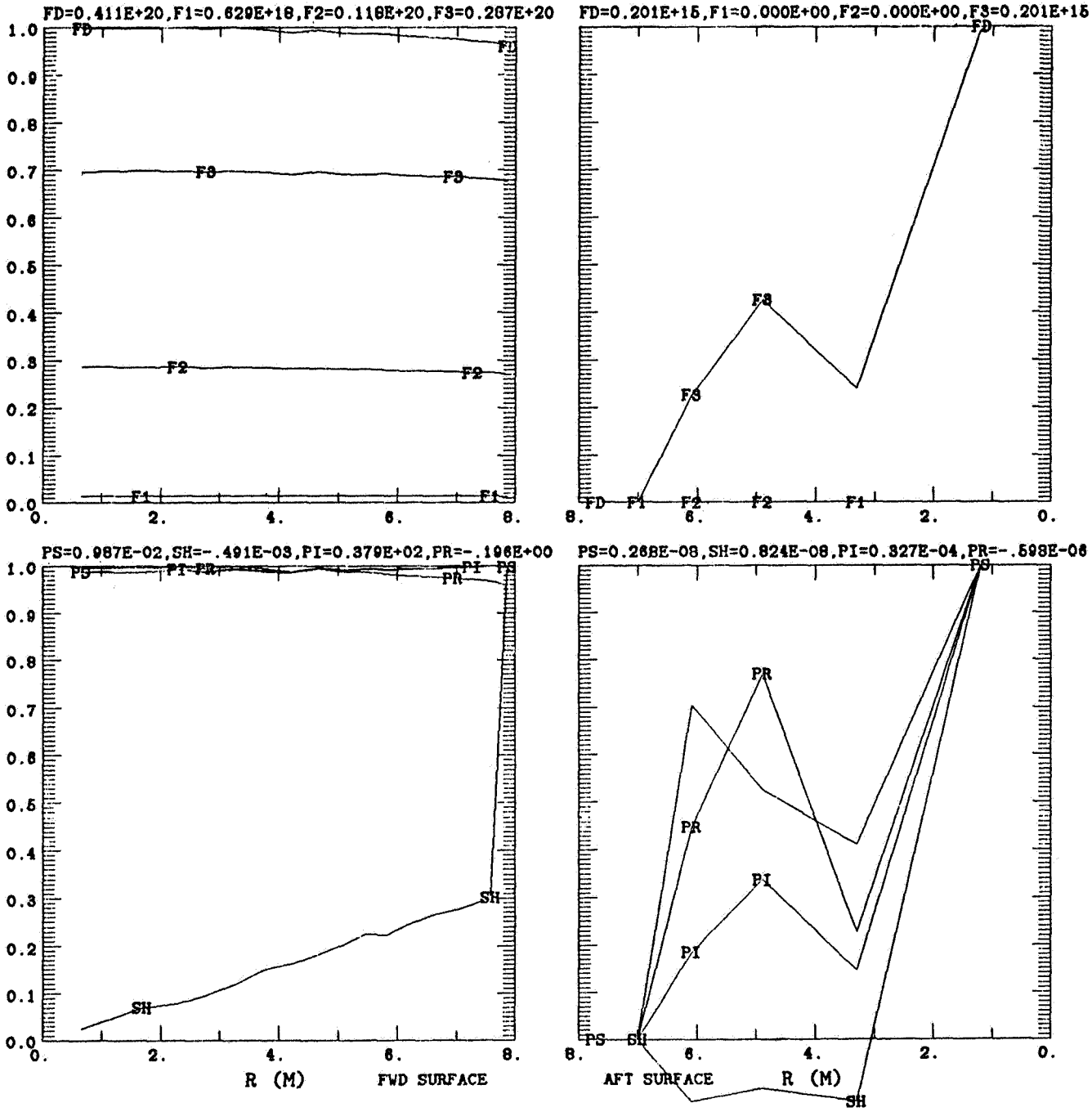

Fig. 5. Gas surface interaction properties. Normalization constants are given above each frame.

TABLE 1. COMPOSITION AND MOLECULAR PROPERTIES

Species	Relative Abundance	Molecular Mass (kg) x 10^{-25}	Rotational Degrees of Freedom	Reference Diameter (m) x 10^{-9}	Reference Temp. (K)	Characteristic Vib. Temp. (K)
1) O_2	0.0142	0.531	2	0.2084	2880	2270
2) N_2	0.2711	0.465	2	0.3105	2880	3390
3) O_1	0.7113	0.265	0	0.2314	2880	-